



Published in final edited form as:

*J Magn Reson Imaging*. 2007 December ; 26(6): 1429–1435. doi:10.1002/jmri.21199.

## Interventional cardiovascular procedures guided by real-time MR imaging: An interactive interface using multiple slices, adaptive projection modes and live 3D renderings

Michael A. Guttman, MS<sup>1</sup>, Cenghizhan Ozturk, MD PhD<sup>2</sup>, Amish N. Raval, MD<sup>2</sup>, Venkatesh K. Raman, MD<sup>2</sup>, Alexander J. Dick, MD<sup>2</sup>, Ranil DeSilva, MBBS PhD<sup>2</sup>, Parag Karmarkar, MS<sup>2</sup>, Robert J. Lederman, MD<sup>2</sup>, and Elliot R. McVeigh, PhD<sup>1</sup>

<sup>1</sup> Laboratory of Cardiac Energetics, Division of Intramural Research, National Heart Lung and Blood Institute, National Institutes of Health, Bethesda, MD

<sup>2</sup> Cardiovascular Branch, Division of Intramural Research, National Heart Lung and Blood Institute, National Institutes of Health, Bethesda, MD

### Abstract

**Purpose**—To develop and test a novel interactive real-time MRI environment that facilitates image-guided cardiovascular interventions.

**Materials and Methods**—Color highlighting of device-mounted receiver coils, accelerated imaging of multiple slices, adaptive projection modes, live 3D renderings and other interactive features are utilized to enhance navigation of devices and targeting of tissue.

**Results**—Images are shown from several catheter-based interventional procedures performed in swine that benefit from this custom interventional MRI interface. These include endograft repair of aortic aneurysm, balloon septostomy of the cardiac interatrial septum, angioplasty and stenting, and endomyocardial cell injection, all using active catheters containing MRI receiver coils.

**Conclusion**—Interactive features not available on standard clinical scanners enhance real-time MRI for guiding cardiovascular interventional procedures.

### Keywords

Interventional MRI; Real-time MRI; Image guided interventions; Catheterization; User Interface

### Introduction

Magnetic resonance imaging (MRI) is a promising real-time (RT) guidance modality for interventional cardiovascular procedures. Although the spatial resolution achievable in MRI is not near that of x-ray techniques, more anatomical detail is available due to increased soft tissue contrast and oblique thin-slice imaging. X-ray computed tomography with contrast enhancement provides this detail, but the excessive radiation dosage is prohibitive. MRI also produces temporal resolution lower than that of x-ray techniques, but demonstrably sufficient to guide catheterization in humans (1). In addition to excellent soft tissue contrast, MRI offers many different ways to produce and process tissue-related signal, thereby affording versatile contrast mechanisms and flexible slice positioning. Pulse sequence

parameters can be changed dynamically during real-time imaging (2,3) to alter the imaging slice or contrast as needed for different stages of an examination or invasive procedure (4). For example, these capabilities have been used for delivery and immediate visualization of myocardial injections of contrast-labeled stem cells (5,6). Multiple parallel or oblique slices may be imaged in rapid succession to provide more complete views of a tortuous blood vessel or other anatomical structure, and these slices can be displayed together in a 3D rendering (7-9). Receiver coils embedded in interventional devices can be used for device tracking (10,11), near-field imaging (12,13), or the coil locations may be visualized by colorizing the images reconstructed from the device coil signals and blending them with grayscale images produced from surface coil signals (7,8,14,15). The color-highlighted images indicate the positions of invasive devices with anatomical context.

Recent work has shown the utility of device-only projection imaging, an interactive imaging mode where slice-selection is turned off and images are produced using only signals from invasive devices (16) for views that resemble x-ray fluoroscopy. This mode can be switched on during scanning for any slice to provide projection views of the entire device, portions of which may be outside the thin-slice imaging plane. An advance we present on this feature is closed-loop control of the projection direction, adaptively reorienting it in response to interactive rotations of the 3D rendering. This adaptively oriented projection navigation (PRONAV) image was displayed with a thin-slice image in a 3D rendering, providing a real-time 3D view of the catheter position and trajectory with respect to the thin-slice image plane. This technique may facilitate the navigation of a device towards a target. Closed-loop control of the MR scanner opens a multitude of possibilities for new features in interactive imaging, since there are many potential methods for synchronizing image acquisition and adjusting imaging parameters. For example, researchers have implemented closed-loop control of the imaging scan plane and/or field-of-view in response to invasive device position and motion (10,17,18).

This report describes a real-time MR imaging system we developed for use in an interventional setting (19). The system has been used by our group in a number of pre-clinical studies in swine, including intramyocardial injection of stem cells (6), endovascular repair of abdominal aortic aneurysms (20), stenting of aortic coarctation (21), recanalization of chronic total occlusions (22), atrial-septal puncture and balloon septostomy (23) and catheterization in humans (24). We describe the features of the system and its potential use in different clinical interventions.

## Materials and Methods

### Imaging System

Clinical MR 1.5T scanners (Sonata with 8 receiver channels, Espree with 18 receiver channels, and Avanto with 32 channels, Siemens Medical Systems, Erlangen, Germany) were modified for sockets communication over Gigabit Ethernet with a Linux workstation (8-CPU, 64-bit, AMD Opteron, HPC Systems, San Jose, CA) running custom software for rapid image reconstruction, display and 3D rendering (7,25). The workstation was connected directly to the image reconstruction computer of the MRI scanner for quick access to the raw MR data. The reconstruction and display software takes advantage of parallel processing by farming out tasks to different threads, which can run concurrently on different CPUs. Threads were created for individual processing of data from each receiver channel, combination of the data, graphical display, communications, and other tasks that could be executed in parallel. Open source packages were used wherever possible: Fast Fourier transforms were performed using the FFTW library (fftw.org), graphics and user interface were implemented using OpenGL and GLUT (opengl.org).

At the beginning of the scan, imaging parameters were sent from the scanner to the workstation for initialization of the reconstruction program. At the end of each image acquisition, a packet of data was sent containing dynamic imaging parameters and the raw MR data. Commands were sent to the scanner in response to user input via the same network interface.

### Pulse Sequence

Steady-state free precession (SSFP, a.k.a. True FISP, b-FFE, FIESTA) (26) was used for rapid, high SNR, consecutive imaging of multiple slices. Imaging parameters were tailored to the experiment; although high frame rates were available, spatial resolution and image quality were always given priority over imaging speed. The imaging frame rate was then increased using variable rate view sharing and/or TSENSE (25,27). Both of these methods accelerate image acquisition by skipping phase encoding lines. For example, at acceleration rate 2, odd and even lines are skipped in alternating acquisitions. For acceleration rate  $N$ , every  $N$ th line is acquired, incrementing the starting line each acquisition. This causes ghosting of moving objects artifacts which TSENSE suppresses using dynamic estimates of the coil sensitivities.

Typical imaging parameters when imaging the heart were: matrix size  $108 \times 192$ , TR/TE=3.84/1.92 ms, bandwidth 1000 Hz/pixel or higher, excitation RF pulse  $\alpha=45$  degrees,  $\frac{3}{4}$  partial phase-encode acquisition with homodyne detection for  $k$ -space filling (28) and acceleration rate 2. For higher quality imaging of more stationary tissues such as peripheral vessels, the parameters were typically changed to  $168 \times 224$  matrix, 800 Hz/pixel bandwidth, full phase-encode acquisition and acceleration rate 2 or 3. Frame rate ranged from 3 to 8 per second, depending on the choice of imaging parameters.

For an acquisition of multiple slices or if magnetization preparation was used (e.g. fat or non-selective saturation), the magnetization was stored longitudinally (along the  $z$ -axis) after each image acquisition using a 'closing' sequence ( $-\alpha/2$ ; gradient spoil) (29), followed by the preparation and an 'opening' sequence (gradient spoil;  $\alpha/2$ ;  $-\alpha$ ; dummy pulses) on the new slice. Fat-selective saturation was achieved by either a typical fat selective RF pulse or one of the quicker off-resonance saturation schemes as described elsewhere (30,31).

The Siemens torso phased-array coil or a custom design surface coil (Nova Medical, Wilmington, MA) was placed on the ventral surface. Spine coils were turned on only when necessary, e.g. for imaging the aorta or some peripheral vessels, otherwise they were turned off to allow us to reduce the FOV and increase spatial resolution. One or two receiver channels were used for device-mounted coils. A total of 4—6 receiver channels were used for data acquisition. The scanner was set up to function normally while MR echo data was simultaneously transferred to the workstation for custom reconstruction and display features. Image reconstruction on the scanner could be turned off in case a high data rate (e.g. from using many receiver channels) was causing it to lag behind image acquisition. Limiting the number of channels was not necessary for image reconstruction on the workstation.

### Interactive Imaging Features

Interactive commands from the workstation user interface were sent to the scanner, which was programmed to react to these commands during imaging. Many interactive features could be controlled by a simple key press or mouse operation without stopping the scanner, and the most frequently used include the following:

- Display each slice in separate windows as well as a 3D rendering where they are shown at their respective locations in space (see Figure 1). This provided simultaneous views of all slices and devices.

- Rotate the 3D rendering for desired viewing angle. This does not affect the imaging planes, but only how they are displayed.
- Apply cut planes to eliminate non-essential data and reduce clutter in the 3D rendering.
- Use non-selective saturation to darken background and isolate T1-shortening contrast agent (see Figure 2).
- Enable device-only projection view on selected slices to show entire device if it exited from the thin slice.
- Change acceleration rate. Typically this is set to the highest value which produces acceptable image quality.
- Change slice position/orientation using the standard scanner slice prescription interface.
- Turn off/on acquisition of selected slices. This was often used when slices were initially prescribed for all stages of the procedure, then only those needed at the time were enabled.
- Display device channels in different colors, blended with grayscale images from surface coils (see Figure 1).
- Adjust brightness of an individual receiver channel. This was often used to change the brightness of an active interventional device.
- Automatic radial sensitivity correction (profile flattening) of axial images from an active (i.e. signal receiving) invasive device. This can be used for vessel imaging (see Figure 3).
- Intensity compression to flatten the device profile in non-axial images (see Figure 4). This can provide better visibility of tissues not immediately adjacent to the device.
- Enable squaring of the device signal magnitude. This is a simple method for sharpening the display of device location (see Figure 5).
- Enable subtraction imaging for enhancing contrast injections.
- Enable cardiac gating. After each trigger, all slices would be acquired and the scanner would wait for the next trigger. This was used to acquire each slice at a consistent cardiac phase.
- Marking of reference points. Reference points are displayed in the 3D rendering and persist until deleted. This was used to mark anatomical features for device positioning (see Figure 1).
- Enable saving of raw data to files. The same program can be used at a later time to review the images with the same or different options for reconstruction or display. Several display and rendering parameters (such as 3D rendering orientation, highlight colors, window positions) were also stored. Post-procedure review therefore could mimic how the images were displayed during the actual procedure.

In adaptive projection navigation (PRONAV) mode, a device-only projection image and at least one thin-slice image were acquired successively and displayed in the 3D rendering. As the user interactively rotated the rendering, the new rendering orientation was repeatedly sent to the scanner, modifying the imaging gradients to reorient the projection direction of the next image normal to the viewing screen. This gave the user the impression of a 3D view of the device from any chosen angle. For quicker response time, acquisition of the thin-slice

image was automatically suspended while the user rotated the rendering, allowing more frequent updates of the projection image. For anatomical context, the thin-slice image was positioned to contain target tissue, myocardium exhibiting post-contrast hyperenhancement. A reference point was placed at a border region of the hyperenhanced tissue to mark the target. The interactive 3D rendering was then used to guide the device towards the target in the thin-slice imaging plane.

### **Invasive Devices**

Several custom made active interventional devices, such as guide-wires and catheters incorporating an active solenoid coil at the distal tip or loopless antenna (32), were used to illustrate the features described above. One such device is an active dual-channel intravascular endograft system (20) for delivery of an endograft in an abdominal aortic aneurysm. A small solenoid coil was mounted at the distal tip and the endograft stent was designed as a loopless antenna. Radial sensitivity correction is demonstrated using an active guide wire designed as a loopless antenna (23). PRONAV is demonstrated using a dual-channel injection catheter designed by S. Smith and G. Scott (6), based on the x-ray compatible Stilleto catheter (Boston Scientific, Inc.), which had an antenna along its shaft and a small coil near the tip, which were shown color-highlighted in the 2D images.

### **Room Setup**

Several displays are used in both rooms to monitor the function of the scanner, external workstation and physiology (19). Team members wore custom-designed communication headsets (Magnacoustics, Atlantic Beach, NY) with noise-cancelling optical microphones (Phone-Or, Or-Yehuda, Israel) to coordinate with each other during a scan for imaging parameter changes, timing during injections, saving data, or to communicate with the patient and nurse on a separate channel. Slice position and orientation changes are adjusted interactively in the graphical prescription interface on the scanner console, which are reflected immediately on the external workstation. An x-ray system is available near the magnet for use during preparation or emergency.

### **Animal Experiments**

Experiments were approved by the institutional animal care and use committee and conducted in accordance with National Institutes of Health guidelines. Miniswine underwent anesthesia induction with atropine, butorphanol, ketamine and xylazine, and maintained under inhaled isoflurane using mechanical ventilation. Heparin 50 units/kg was administered after percutaneous vascular access. Survival experiments were conducted using aseptic technique.

### **Results**

Some of the important features of the system are illustrated in Figure 1. This figure shows a screen capture on the external workstation during inflation of a balloon placed in the abdominal aorta. The multiple slices were acquired in succession and displayed at their respective locations on the 3D rendering. Images from the active guide wire inside the balloon catheter are reconstructed separately from that of the surface coils, color highlighted and blended. The ends of the balloon were marked on the images and displayed in the 3D rendering (arrows pointing to cyan and yellow dots, respectively). The device position was clearly seen, facilitating wire navigation and balloon placement using real-time MRI guidance.

Figure 2 shows the advantages of dynamically changing imaging contrast in catheter-based procedures. In this procedure, an angioplasty balloon catheter is used to expand an atrial

septal puncture (23). A guide-wire incorporating a loopless antenna, was placed in the lumen of the catheter for visualization of the catheter trajectory and increased sensitivity to signal from fluid in the balloon. Before balloon inflation with Gd-DTPA contrast agent, a button was pressed to activate background suppression using a non-selective saturation pulse before each image acquisition. As shown in the figure, the inflated balloon is easily seen against the suppressed background.

The next figures show how the sensitivity profile of the guide-wire antenna may be flattened for imaging with the active device or sharpened for visualization of the device position. The sensitivity of a loopless antenna decreases with the radial distance from the device as  $1/r$  (32). Thus if the device position is known, the signal intensity may be flattened using multiplication by  $r$  at each pixel. In an axial orientation, it is easy to automatically find the device position by searching for the location of maximal signal intensity in the image reconstructed by the device signal alone. Figure 3 and Movie 1 illustrate how this is done in real-time, allowing the device to be used for imaging. Only a small region around the device is displayed, since the SNR decreases rapidly with distance from the device.

In non-axial views (e.g. Figure 4a), parts of the device may be in plane while others may be partially or completely out of plane. This makes  $1/r$  correction more difficult since the entire device trajectory must be automatically estimated, which can be accomplished using projection imaging from multiple angles. Alternatively, a simple way to achieve a flattening effect is to use a mathematical operator with logarithmic behavior to compress the device intensity, similar to what is commonly done with ultrasound images (33). In Figure 4b, a square-root operator was used to compress the brightness. This brightens the weaker signals, such as those further away from the device. It does not perform as well as  $1/r$  correction, but allows us to see additional image details without the computation required to estimate device trajectory in non-axial views.

For visualizing device position, sharpening of the device profile is sometimes desirable. For this effect, we did the opposite of what was done for device imaging and used the square of the device intensity, as shown in Figure 5. We find this effect most useful when the device is in-plane and usually disable it when using projection imaging or moving the slice to find the device. All of these flattening and sharpening effects may be interactively enabled or disabled during a scan.

Figure 7 and Movie 2 demonstrate PRONAV for real-time 3D visualization of an active catheter and navigation towards infarct border tissue in a 2D image plane, swine model (6). Projection imaging allowed continuous visualization of the device with 3D effect when the rendering was rotated. Targeting of infarct borders was enhanced since regions of reduced cardiac function and delayed hyperenhancement (post-contrast) were observable in the thin-slice image. The adaptive projection image gave 3D feedback about device trajectory with respect to the thin-slice image. This mode simplified catheter steering toward target tissue in the imaging plane.

## Discussion

We have developed an interactive real-time MR imaging environment for use in interventional procedures. Many features were implemented that exploit the advantages of MRI such as enhancing visualization of receiver coils mounted on invasive devices, providing multiple oblique slices which are easily adjusted, rendering all slices and landmarks in 3D, accelerated imaging and projection imaging modes to see the entire trajectory of an active device.



Real-time imaging of multiple oblique slices offers many potential advantages. Different views of complicated anatomy may be simultaneously displayed and individual slices can be interactively turned on or off during a scan as needed. Another important use would be to provide continuous monitoring of function (e.g. heart motion) in one view during an intervention requiring a different view. At the intersections of imaging planes, saturation can result in a thin line, which is faintly visible in Figure 1. There is an associated reduction of SNR at this line, but not severe enough to hamper visualization in the procedures we have tested thus far. The saturation line can help by providing a certain indicator of intersecting imaging plane position, and we sometimes use this for fine adjustment of plane positions. In our experience, this line is thicker when using a spoiled gradient recalled echo imaging sequence.

High performance hardware was used to minimize image reconstruction latency, which we estimate at approximately ¼ second. As reported, typical frame rates ranged from 3 to 8 per second, depending on choice of parameters. The reconstruction system was able to sustain this frame rate regardless of the number of channels in use. Much higher frame rates, in excess of 30 per second, were sustainable by the system using small matrix (e.g. 64×128), view sharing and 8 channels. This small matrix does not result in adequate image quality, but was useful to gauge the limits of the system. As of this writing, better raw data throughput and a faster reconstruction computer are required to handle real-time processing of 32-channel data with high acceleration rates and larger matrix.

Features were chosen for implementation based on the specific needs of different invasive procedures performed over the last several years at our institution. Prior to scanning, we discuss which features will be in use. During the experiment the interventionalist communicates to the console operator which features or slices to enable or disable, or sometimes the operator anticipates what is needed. Human experience has been limited due to difficulty obtaining approval for use of custom devices. Further advancements will incorporate more advanced real-time volume rendering modes, other closed-loop control modes such as PRONAV and slices which follow device position (18). Imaging suites incorporating these capabilities could benefit a variety of cardiovascular and non-cardiovascular interventional procedures using real-time MRI guidance.

## Supplementary Material

Refer to Web version on PubMed Central for supplementary material.

## Acknowledgments

The authors express their thanks to Joni Taylor, Katherine Hope and Victor Wright for their support during this development.

**Grant Support:** This work was supported by NIH Z01-HL005062-04 (RJL) and NIH Z01-HL004608-06 (ERM).

## References

1. Razavi R, Hill DL, Keevil SF, et al. Cardiac catheterisation guided by MRI in children and adults with congenital heart disease. *Lancet* 2003;362:1877–1882. [PubMed: 14667742]
2. Holsinger AE, Wright RC, Riederer SJ, Farzaneh F, Grimm RC, Maier JK. Real-time interactive magnetic resonance imaging. *Magn Reson Med* 1990;14:547–553. [PubMed: 2355836]
3. Hardy CJ, Darrow RD, Nieters EJ, et al. Real-time acquisition, display, and interactive graphic control of NMR cardiac profiles and images. *Magn Reson Med* 1993;29:667–673. [PubMed: 8505903]

4. Lederman RJ, Guttman MA, Peters DC, et al. Catheter-based endomyocardial injection with real-time magnetic resonance imaging. *Circulation* 2002;105:1282–1284. [PubMed: 11901036]
5. Kraitchman DL, Heldman AW, Atalar E, et al. In vivo magnetic resonance imaging of mesenchymal stem cells in myocardial infarction. *Circulation* 2003;107:2290–2293. [PubMed: 12732608]
6. Dick AJ, Guttman MA, Raman VK, et al. Magnetic resonance fluoroscopy allows targeted delivery of mesenchymal stem cells to infarct borders in Swine. *Circulation* 2003;108:2899–2904. [PubMed: 14656911]
7. Guttman MA, Lederman RJ, Sorger JM, McVeigh ER. Real-time volume rendered MRI for interventional guidance. *J Cardiovasc Magn Reson* 2002;4:431–442. [PubMed: 12549231]
8. Quick HH, Kuehl H, Kaiser G, et al. Interventional MRA using actively visualized catheters, TrueFISP, and real-time image fusion. *Magn Reson Med* 2003;49:129–137. [PubMed: 12509828]
9. Blinded. ISMRM. Miami: 2005. Interactive Frontend (IFE): A Platform for Graphical MR Scanner Control and Scan Automation.
10. Zuehlsdorff S, Umatham R, Volz S, et al. MR coil design for simultaneous tip tracking and curvature delineation of a catheter. *Magn Reson Med* 2004;52:214–218. [PubMed: 15236390]
11. Feng L, Dumoulin CL, Dashnaw S, et al. Transfemoral catheterization of carotid arteries with real-time MR imaging guidance in pigs. *Radiology* 2005;234:551–557. [PubMed: 15591433]
12. Atalar E, Kraitchman DL, Carkhuff B, et al. Catheter-tracking FOV MR fluoroscopy. *Magn Reson Med* 1998;40:865–872. [PubMed: 9840831]
13. Hillenbrand CM, Elgort DR, Wong EY, et al. Active device tracking and high-resolution intravascular MRI using a novel catheter-based, opposed-solenoid phased array coil. *Magn Reson Med* 2004;51:668–675. [PubMed: 15065238]
14. Serfaty JM, Yang X, Aksit P, Quick HH, Solaiyappan M, Atalar E. Toward MRI-guided coronary catheterization: visualization of guiding catheters, guidewires, and anatomy in real time. *J Magn Reson Imaging* 2000;12:590–594. [PubMed: 11042641]
15. Aksit P, Derbyshire JA, Serfaty JM, Atalar E. Multiple field of view MR fluoroscopy. *Magn Reson Med* 2002;47:53–60. [PubMed: 11754442]
16. Peters DC, Lederman RJ, Dick AJ, et al. Undersampled projection reconstruction for active catheter imaging with adaptable temporal resolution and catheter-only views. *Magn Reson Med* 2003;49:216–222. [PubMed: 12541240]
17. Derbyshire JA, Wright GA, Henkelman RM, Hinks RS. Dynamic scan-plane tracking using MR position monitoring. *J Magn Reson Imaging* 1998;8:924–932. [PubMed: 9702895]
18. Elgort DR, Wong EY, Hillenbrand CM, Wacker FK, Lewin JS, Duerk JL. Real-time catheter tracking and adaptive imaging. *J Magn Reson Imaging* 2003;18:621–626. [PubMed: 14579407]
19. Guttman, MA.; Lederman, R.J.; McVeigh, ER. The cardiovascular interventional MRI suite: design considerations. In: Lardo; Fayad; Fuster; Chronos, editors. *Cardiovascular Magnetic Resonance: Established and Emerging Applications*. London: Martin Dunitz; 2003.
20. Raman VK, Karmarkar PV, Guttman MA, et al. Real-time magnetic resonance-guided endovascular repair of experimental abdominal aortic aneurysm in swine. *J Am Coll Cardiol* 2005;45:2069–2077. [PubMed: 15963411]
21. Raval AN, Telep JD, Guttman MA, et al. Real-time magnetic resonance imaging-guided stenting of aortic coarctation with commercially available catheter devices in Swine. *Circulation* 2005;112:699–706. [PubMed: 16043639]
22. Raval AN, Karmarkar PV, Guttman MA, et al. Real-Time MRI-Guided Endovascular Recanalization of Chronic Total Arterial Occlusion in a Swine Model. *Circulation* 2006;113:1101–1107. [PubMed: 16490819]
23. Raval AN, Karmarkar PV, Guttman MA, et al. Real-Time MRI Guided Atrial Septal Puncture and Balloon Septostomy in Swine. *Catheterization and Cardiovascular Interventions* 2006;67:637–43. [PubMed: 16532499]
24. Dick AJ, Raman VK, Raval AN, et al. Invasive human magnetic resonance imaging: Feasibility during revascularization in a combined XMR suite. *Catheter Cardiovasc Interv* 2005;64:265–274. [PubMed: 15736247]



25. Guttman MA, Kellman P, Dick AJ, Lederman RJ, McVeigh ER. Real-time accelerated interactive MRI with adaptive TSENSE and UNFOLD. *Magn Reson Med* 2003;50:315–321. [PubMed: 12876708]
26. Oppelt A, Graumann R, Barfuß H, Fischer H, Hartl W, Scajor W. FISP—A New Fast MRI Sequence. *Electromedica* 1986;54:15–18.
27. Kellman P, Epstein FH, McVeigh ER. Adaptive sensitivity encoding incorporating temporal filtering (TSENSE). *Magn Reson Med* 2001;45:846–852. [PubMed: 11323811]
28. Noll DC, Nishimura DG, Macovski A. Homodyne Detection In Magnetic Resonance Imaging. *IEEE Trans Med Imag* 1991;10:154–163.
29. Scheffler K, Heid O, Hennig J. Magnetization preparation during the steady state: fat-saturated 3D TrueFISP. *Magn Reson Med* 2001;45:1075–1080. [PubMed: 11378886]
30. Derbyshire JA, Herzka DA, McVeigh ER. S5FP: Spectrally selective suppression with steady state free precession. *Magn Reson Med* 2005;54:918–928. [PubMed: 16155880]
31. Santos, JM.; Hargreaves, BA.; Nayak, KS.; Pauly, JM. Real-Time Fat Suppressed SSFP. *Proc 11th ISMRM; Toronto. 2003. p. 982*
32. Ocali O, Atalar E. Intravascular magnetic resonance imaging using a loopless catheter antenna. *Magn Reson Med* 1997;37:112–118. [PubMed: 8978639]
33. Christensen, DA. *Ultrasonic bioinstrumentation*. New York: John Wiley & Sons; 1988.

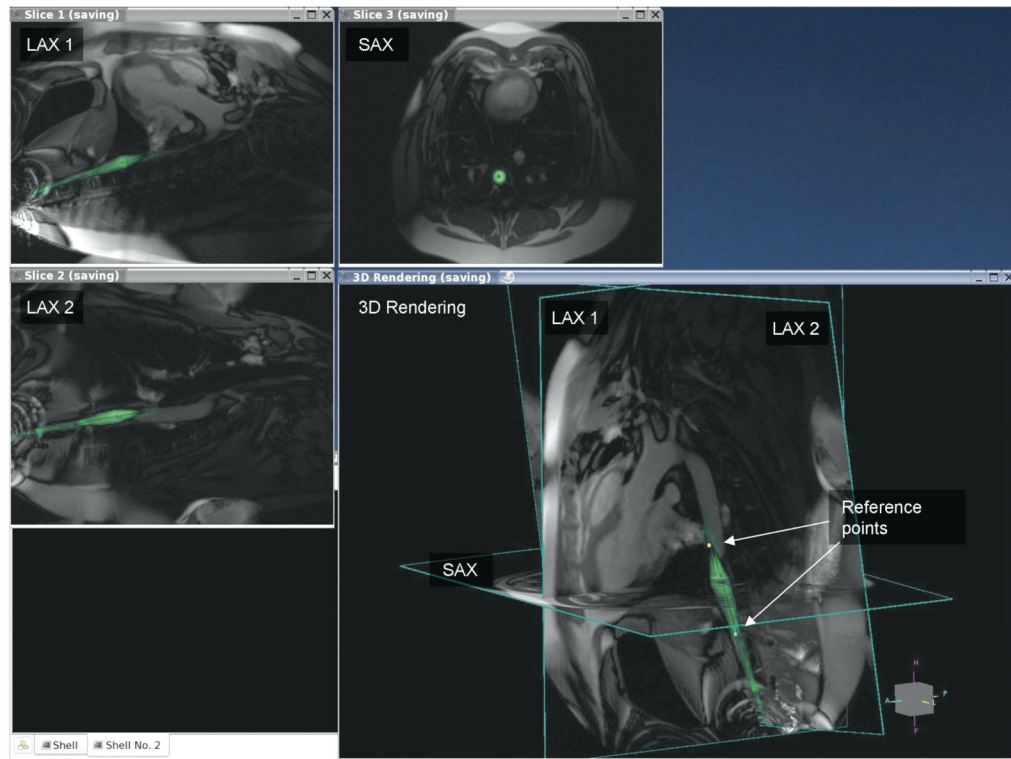


**Figure 1.**

This is a multi-slice real-time scan of a balloon inflation within a swine abdominal aorta. Two long axis views and one short axis view intersect the vessel. The arrows point to two dots in the 3D rendering which mark the ends of the balloon. The green color is from signal obtained from an active guide wire placed within the balloon catheter.

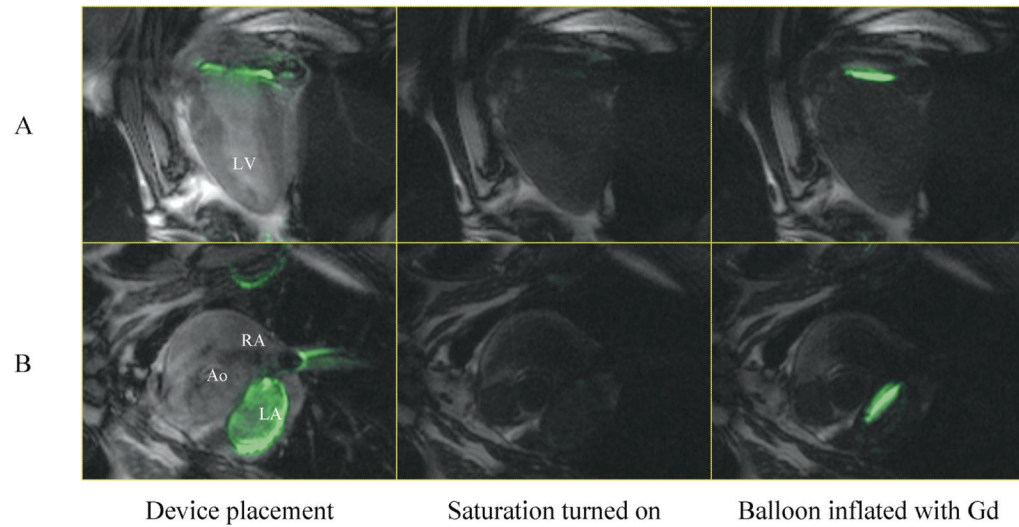


**Figure 2.** The use of interactive non-selective saturation is shown during an atrial-septal puncture and septostomy experiment. The active guide-wire is color-highlighted in green and blended with background long-axis (A) and short-axis (B) views. The first column shows the device across the septum and coiled in the left atrium. Saturation is enabled in the second and third columns, with the Gd-filled balloon clearly visible in the third column.

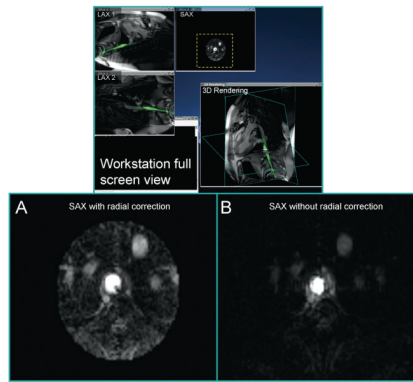


**Figure 3.** Radial correction (flattening) of the axial device profile is performed in real-time to enhance device image interpretation. The close-ups of slice 3 in (A) and (B) compare reconstruction with and without radial correction, respectively. This corrected image is shown in a 2D window as well as the 3D rendering (B).

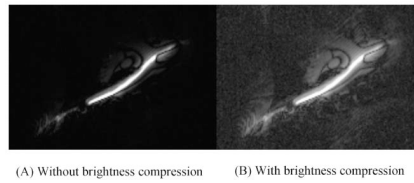


**Figure 4.**

This figure shows the effect of intensity compression using a square-root operator on a non-axial view of the active device. An active guide wire is shown in the descending aorta, entering a carotid artery. The intensity compression produces an effect that is qualitatively similar to radial correction in an axial view. The surrounding tissue further from the device becomes more visible.

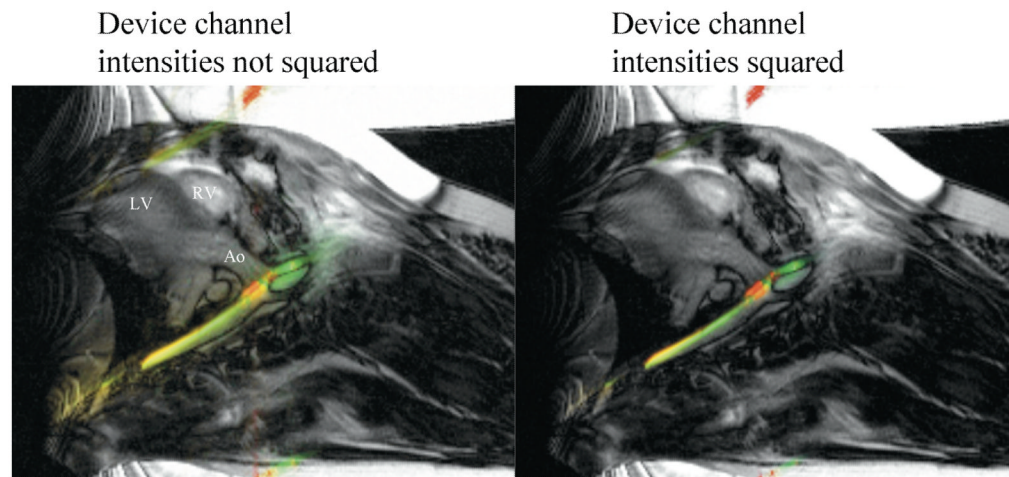


**Figure 5.**

To sharpen the device profile, we perform the opposite of compression using a square operator on the device image intensity. This sharpening allows more precise visualization of the device location. The active guide wire is highlighted in green, and small coils on a guiding catheter are highlighted in red. The active devices are seen in the descending aorta, entering a carotid artery.



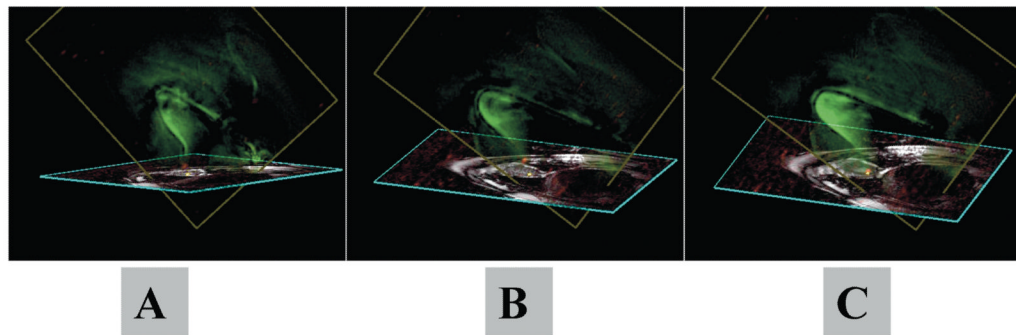


**Figure 6.**

Adaptive projection navigation (PRONAV) is illustrated for real-time 3D visualization of an active catheter and navigation towards infarct border tissue in a 2D image plane. This is an injection catheter containing two receivers: a small coil at the tip (red) and a loopless antenna along the shaft (green). A yellow dot marks the target tissue. The rendering is manually rotated during the scan to see the device trajectory from different angles, giving a 3D effect.